THE JOURNAL OF PHYSICAL CHEMISTRY Letters

Letter

Cite This: J. Phys. Chem. Lett. 2019, 10, 4003−4009

pubs.acs.org/JPCL

Photolytic Aging of Secondary Organic Aerosol: Evidence for a Substantial Photo-Recalcitrant Fraction

Rachel E. O'Brien*,†,‡ and Jesse H. Kroll‡

†Department of Chemistry, College of William and Mary, Williamsburg, Virginia 23185, United States

‡Department of Civil and Environmental Engineering, Massachusetts Institute of Technology, Cambridge, Massachusetts 02139, United States

Supporting Information

ABSTRACT: Photolytic aging has been proposed as a major mass loss mechanism for atmospheric secondary organic aerosol (SOA). However, estimated mass loss rates vary by orders of magnitude, and their impacts on modeled SOA loadings and properties are highly uncertain. In this study, photolysis rates and composition changes of α-pinene SOA are analyzed *in situ* over multiple days in an environmental chamber. After an initial exponential decay ($\tau \sim 22$ h), the mass loss rate slows dramatically, with more than ~70−90% of the SOA particulate mass undergoing an essentially negligible photolytic degradation. Scaled to ambient conditions, SOA undergoes rapid photolysis over only its first day in the atmosphere; beyond this, the remaining SOA is photo-recalcitrant, and photolysis ceases to be a major sink compared to wet deposition time scales. Thus, extrapolation of the initial photolysis loss rate to the entire aerosol mass may significantly overestimate the role of photolysis in the removal of atmospheric SOA.

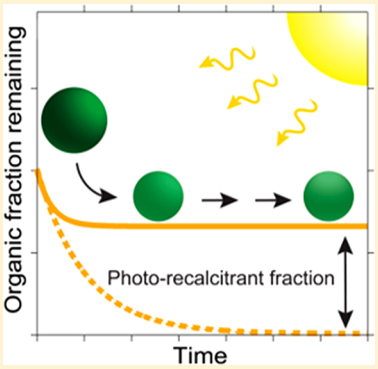

Secondary organic aerosol (SOA), formed in the atmosphere through photochemical oxidation of hydrocarbons, has effects on both climate and human health. However, our ability to accurately model the atmospheric life cycle of SOA is limited by our understanding of its complex formation, aging, and loss processes. A major area of focus has been on mechanisms of SOA formation, with far less study of SOA sinks. In addition to standard physical loss processes (wet and dry deposition), SOA may be degraded chemically; recent modeling work has shown that inclusion of chemical loss processes can improve model−measurement discrepancies.[1,2]

Chemical loss processes for SOA involve fragmentation reactions followed by evaporation of volatile products, processes that may be initiated by heterogeneous oxidation,[3] aqueous-phase oxidation,[4] and photolysis.[5−8] A number of laboratory studies have demonstrated the importance of this last channel, the photolytic loss of SOA by ultraviolet (UV) light.[5,7−11] Recently, a modeling study by Hodzic et al. demonstrated that photolysis may be a major sink for atmospheric SOA, with photolytic lifetimes of ~1 week, which is comparable to the lifetime for wet deposition.[12] However, the photolytic mass loss rate of SOA is still very poorly constrained. Laboratory studies examining photolytic loss rates in chambers and flow tubes have reported rates spanning orders of magnitude, with estimated atmospheric lifetimes of anywhere from hours to days.[5−8]

Currently, photolytic lifetimes are determined by applying initial measured photolysis loss rates to the entire SOA mass. However, only a few oxygen-containing functional groups (such as carbonyls, nitrates, and peroxides) are chromophores that can absorb solar radiation in the wavelength ranges that reach the troposphere ($\lambda \gtrsim 290$ nm). Applying a single photolysis mass loss rate assumes that all SOA molecules have enough of these chromophores to completely fragment and/or volatilize the entire OA mass. This also neglects the possibility that photolysis may destroy the chromophores, thereby photobleaching the SOA and preventing further photolysis.[13−16] The effects of these factors on photolysis-driven SOA loss rates over extended time periods have not yet been explored.

To investigate how photolysis affects the mass of SOA over extended atmospheric lifetimes, we present results from α-pinene/ozone SOA photolysis over time scales of ~1−2 days. Experiments were carried out in a 7.5 m^3 environmental chamber equipped with UVA lights at low relative humidity (RH <5%).[17] Full experimental details are available in the Supporting Information. Briefly, excess ozone ($[O_3]_0 > 500$ ppb) was added to the chamber filled with 80−120 ppb α-pinene and ammonium sulfate seed particles, as well as hexafluoropropylene (400 ppm) as an OH scavenger. The SOA mass concentration was measured in real time using a high resolution time-of-flight aerosol mass spectrometer (AMS).[18] The ratio of organic to sulfate mass concentrations (Org/SO_4) was used to quantify organic particulate mass because it accounts for particle losses due to deposition and dilution, as well as changes in AMS collection efficiency. After ~5 h, the mixture was exposed to UVA lights with total irradiation times of 30−40 h or kept unilluminated for control

Received: May 17, 2019
Accepted: July 2, 2019
Published: July 2, 2019

DOI: 10.1021/acs.jpclett.9b01417
J. Phys. Chem. Lett. 2019, 10, 4003−4009

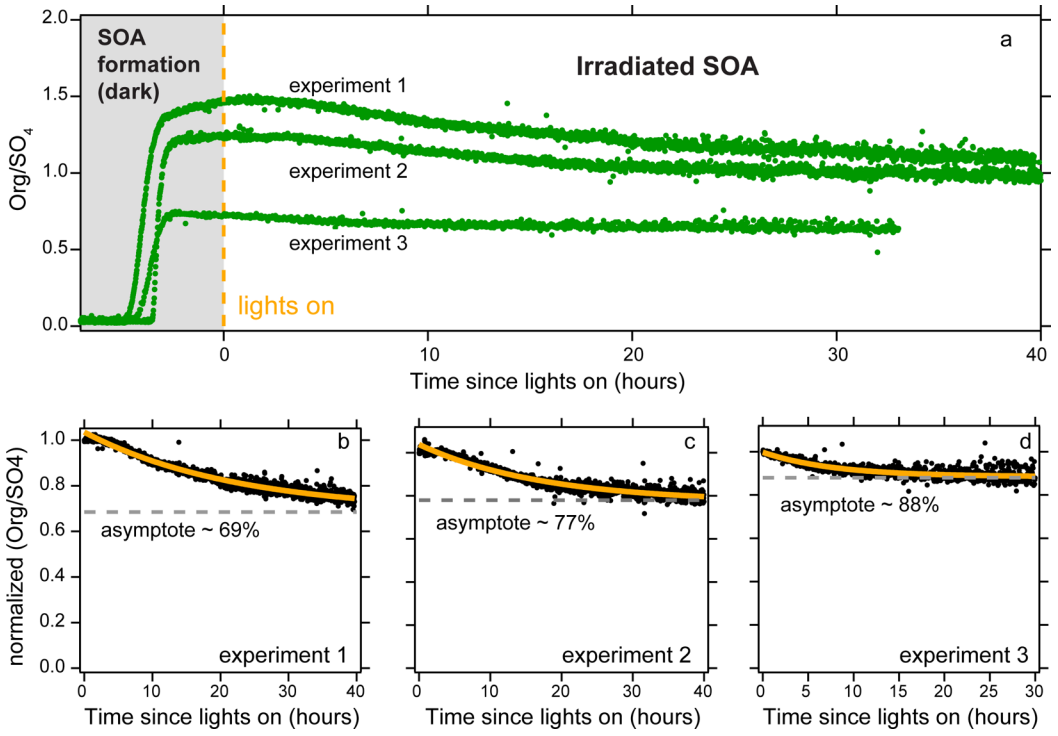

Figure 1. Organic particulate mass vs time for photolysis experiments at three different initial Org/SO_4 ratios. (a) Time traces for Org/SO_4 in the chamber for all three experiments. The vertical line at 0 h (t_0) indicates chamber lights on for the photolysis experiment. (b–d) Organic fractions remaining (normalized Org/SO_4) as a function of irradiation time. A single exponential with a y-offset (highlighted as asymptotes in panels b–d) is fit to the data.

(dark) experiments. The NO_2 photolysis rate (J_{NO_2}), a measure of UV intensity, is $\sim 1.3 \times 10^{-3}$ s^{-1}, slightly lower than average wintertime values at midlatitudes and substantially lower than the value (8.1×10^{-3} s^{-1}) used by Hodzic et al. to model SOA photolytic loss globally.[12] Irradiation likely involves photolysis in the particle and gas phases and in the particle phase may involve both direct and indirect photolysis; here, we investigate photolytic mass loss of SOA as a whole and do not distinguish between these different photolytic processes. We note, however, that any chemical changes observed are unlikely to arise from gas-phase OH, due to the presence of the OH scavenger.

Figure 1a shows the time series for three UV experiments with different initial Org/SO_4 ratios. When the lights were turned on, the Org/SO_4 ratio decreased, indicating a loss of organic mass from the particles with UVA irradiation. Replicate dark experiments did not exhibit this decrease, as the Org/SO_4 ratio was either constant or increased slightly (Figure S1). The photolytic loss rate of particulate organic mass is evaluated by normalizing the Org/SO_4 ratio to the value at time zero (lights on) and fitting an exponential decay (Figure 1b–d and Table 1). In all cases, the mass did not decay to zero but rather to a value corresponding to approximately ~70–90% of the initial mass. The offsets represent a "photo-recalcitrant" fraction of OA, particle mass that does not show measurable photolytic decay. In reality, the photo-recalcitrant fraction may also be undergoing slow photolytic degradation, but over the time scales of these experiments (irradiation for 30–40 h), the rates of such longer time scale processes cannot be determined.

The shapes of the curves in Figure 1 are consistent with photobleaching of SOA; mass loss occurs until the chromophores are lost and only the photo-recalcitrant fraction remains. SOA from α-pinene formed under low-NO_x conditions is a mixture of highly oxidized molecules (HOMs) along with other semivolatile and lower-volatility products, many of which likely contain carbonyls and peroxides.[5,19−23] These functional groups are chromophores that can be lost to either photofragmentation or chemical loss processes. Photobleaching has been observed for brown carbon aerosol in both the field and the laboratory[13−15,24,25] and likely occurs here as chromophores are either destroyed or lost to the gas phase during fragmentation. While the functional group distribution was not characterized in this study, we note that it is likely that a large fraction of α-pinene SOA molecules do not contain chromophores. For example, pinic acid, a major product of α-pinene ozonolysis, includes only acid groups and thus is unlikely to absorb appreciably in the UV.[26] Thus, the photo-recalcitrant fraction is likely a mixture of molecules that

Table 1. Fitting and Simulated Variables for Mass Loss and Oxidation State Changes

variable	experiment 1[a]	experiment 2[a]	experiment 3[a]
recalcitrant fraction of OA (f_R)	0.69 ± 0.003	0.77 ± 0.004	0.88 ± 0.003
time scale for photolytic loss of OA [τ_{OA} (h)]	22 ± 0.4	18 ± 0.7	8 ± 0.9
recalcitrant fraction of carbon (f_R)	0.68 ± 0.002	0.71 ± 0.003	0.82 ± 0.002
time scale for photolytic loss of carbon [τ_C (h)]	18 ± 0.2	18 ± 0.4	8 ± 0.4
chromophore/molecule (c_{pM})	1.4	1.3	0.7
carbon-normalized quantum yield (ϕ)	3.0	2.8	1.5

[a]Coefficients ± 1σ.

DOI: 10.1021/acs.jpclett.9b01417
J. Phys. Chem. Lett. 2019, 10, 4003−4009

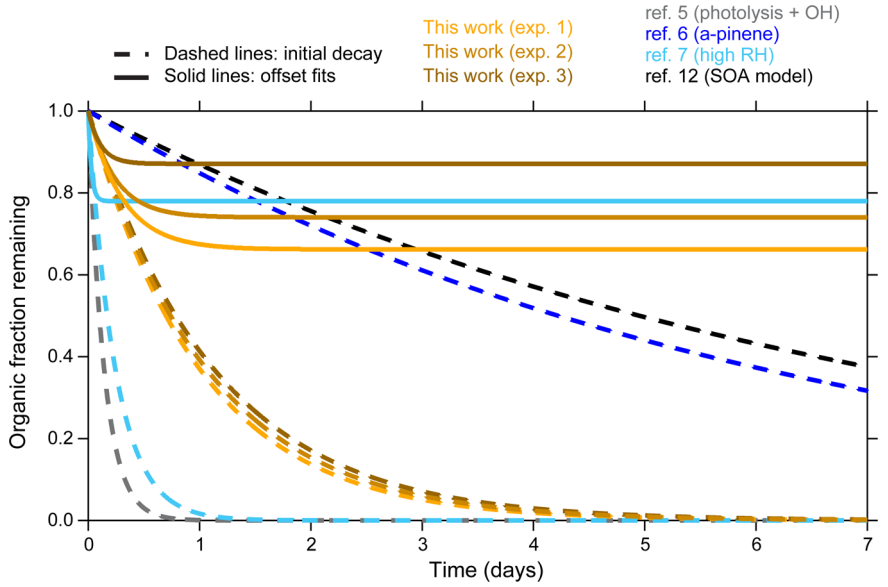

Figure 2. Organic fractions remaining extrapolated out to 1 week in the atmosphere using lifetimes from these experiments, previous SOA photolysis experiments, and models. Two fits for data from the experiments presented here are shown, the τ applied as an exponential decay (dashed lines) and the exponential fit with a y-offset (solid lines). For Wong et al.,[7] the exponential offset fitting was applied to the published data (Figure S2).

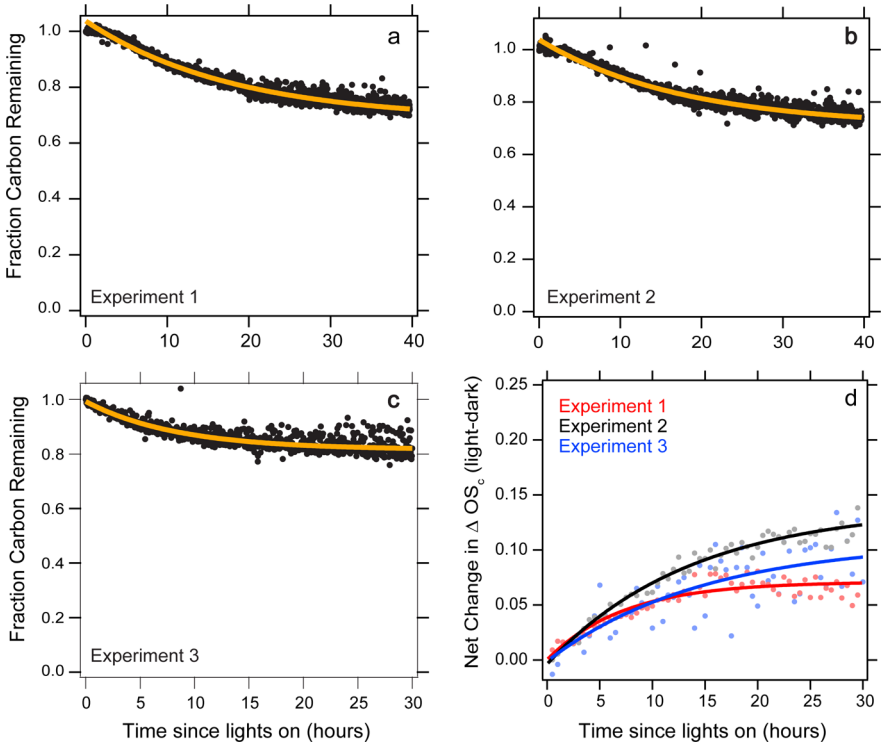

Figure 3. Chemical changes as a function of photolytic aging. (a–c) Carbon fraction remaining (f_C) vs time in the chamber with the exponential and model fits (yellow line). (d) Net (light–dark) $\Delta\overline{OS}_C$ vs chamber time. The $\Delta\overline{OS}_C$ data are plotted using 30 min averages.

are not photoactive as well as non-absorbing products of photolysis that remain in the particles after photobleaching.

The assumption that all of the SOA mass is photolabile has a large impact on the calculated mass loss over the course of the particle's atmospheric lifetime (~1 week). Figure 2 shows estimates of mass loss rates, from both the study presented here and previous work, extrapolated out to 1 week of atmospheric aging. The rate constants are all scaled to the average atmospheric J_{NO_2} used by Hodzic et al. (J_{NO_2} = 8.1 × 10^{-3} s^{-1}), who estimated J_{SOA} to be 0.04% of J_{NO_2} and used this to estimate SOA lifetimes with respect to photolysis in the atmosphere.[12] Dashed lines show SOA decays estimated by assuming that initial photolysis rates apply to the entire particulate organic mass; these rates are taken from the initial decays in the present experiment (orange/brown lines) as well as from previously measured[5−7] and estimated[12] photolysis loss rates (gray, dark blue, light blue, and black lines). Use of

DOI: 10.1021/acs.jpclett.9b01417
J. Phys. Chem. Lett. 2019, 10, 4003−4009

the initial loss rates measured in the experiments presented here would imply that complete loss of particulate organic material (via fragmentation and volatilization) occurs after 4 days; this is intermediate to results from other studies, which suggest complete loss after anywhere from half a day to more than 1 week. Some of this variability likely arises from experimental differences in the systems studied (e.g., RH or light source used). Regardless, in all cases, the use of the initial photolytic rate implies a photolytic lifetime that is comparable to or much faster than rates of wet deposition.

However, the longer time scales in our chamber experiments (Figure 1) show that this initial photolytic loss rate lasts for only ∼1 day in the atmosphere, after which little photolytic SOA mass loss occurs (solid orange/brown lines). One other laboratory study has also shown a leveling off at longer time scales;[7] when exponential offset fits are applied to their data (Figure S2), a similar photo-recalcitrant fraction is determined (solid light blue line). Those experiments were performed at an elevated relative humidity (85% RH), so the recalcitrant fraction is not expected to be entirely due to a lack of photolysis in high-viscosity material.[27,28] The similarity in results between these two sets of experiments, despite differences in reaction conditions (photolysis wavelength and RH), suggests that the observed behavior is a general feature of α-pinene SOA. Some fraction is initially lost via photolysis, but a substantial fraction is photo-recalcitrant and will remain relatively unaffected by photolysis over longer time scales.

While the number of experiments is limited, the fraction of photo-recalcitrant OA appears to increase as the Org/SO_4 ratio decreases (Figures 1 and 2 and Table 1), indicating that differences in partitioning or SOA formation reactions[29−32] possibly play an important role in the fraction of photolabile material present in α-pinene SOA. The OA concentrations here are generally higher than ambient, and thus, care should be taken when comparing chamber results and when extrapolating to ambient systems. Specifically, a simple extrapolation of this general trend to atmospheric OA loadings would suggest a 100% photo-recalcitrant fraction in the atmosphere. However, this seems unlikely as chromophores such as carbonyls, peroxides, nitrate esters, etc., are known components of atmospheric OA.[33,34]

Additional insights into α-pinene SOA photolysis can be gained by analyzing changes in the elemental composition as a function of time. Figure 3 shows trends in the fraction of carbon remaining (f_C) and the carbon oxidation state ($\Delta\overline{OS}_C$),[35] metrics that have been used to describe other aerosol aging processes such as heterogeneous oxidation.[36] f_C was calculated from the total SOA mass and the elemental ratios (O/C and H/C) measured by the AMS.[3] In Figure 3, f_C is normalized to the carbon concentration when the lights were turned on (t_0). $\Delta\overline{OS}_C$ is the difference between the carbon oxidation state (2O/C−H/C) at time t and at t_0, with a subtraction of the time-dependent $\Delta\overline{OS}_C$ for the corresponding dark experiment. This dark subtraction was carried out because a small increase in $\overline{OS}_C$ was observed in the dark (Figure S3), likely due to "ripening" processes occurring as a result of dilution and/or slow reactions of peroxides or other reactive components.[23,37]

In all experiments, photolysis leads to a loss of particulate carbon (decrease in f_C) and a net increase in oxidation state (Figure 3), which is qualitatively similar to heterogeneous and aqueous aging.[3,4] The carbon fraction remaining as a function of time (Figure 3a−c and Table 1) follows a trend similar to that of the total organic mass (Figure 1) with an exponential decay that reaches an asymptote at ∼70−80% carbon remaining. The relatively small net change in the oxidation state (Figure 3d) is consistent with a balance between functional group addition and the volatilization of small oxidized fragments (such as acetone, formaldehyde, and carbon monoxide).[6,19] The differences observed among the three experiments are likely due to variations in the fragments produced, the chemistry that occurs following fragmentation, and differences in the partitioning of both the fragments and SOA components during the experiments.

The carbon loss data in Figure 3a−c can be interpreted in terms of key parameters of the photolysis system. The data are fit to an exponential function (dashed lines) similar to the one used to fit the organic mass loss (Figure 1):

$$f_C = f_R + f_L e^{-t/\tau} = f_R + (1 - f_R)e^{-t/\tau} \quad (1)$$

where f_C is the simulated carbon fraction remaining as a function of time, f_R is the recalcitrant carbon fraction, f_L is the labile fraction (which equals $1 - f_R$), and τ is the lifetime against loss due to photolysis. The labile fraction corresponds to the particulate organic carbon that is lost when all chromophores have absorbed light and released organic carbon fragments to the gas phase; hence, it is a function of the abundance of chromophores and the amount of carbon lost per photolysis reaction:

$$f_L = c_{pM} \times C_{frag}/C_{tot} \quad (2)$$

where c_{pM} is the average number of chromophores per molecule, C_{frag} is the average number of carbon atoms lost to the gas phase per photolysis event (equal to the average carbon number of the volatile fragments), and C_{tot} is the total number of carbons in the molecule.

Lifetime τ is the inverse of photolysis rate constant J of the SOA as a whole:

$$\frac{1}{\tau} = J \cong \phi\left(\frac{1}{c_{pM}} \times \frac{1}{C_{frag}}\right)\int_{\lambda_1}^{\lambda_2} \sigma(\lambda)I(\lambda)\,d\lambda \quad (3)$$

where σ is the average absorption cross section (cm^2 $molecule^{-1}$) of chromophore-containing molecules within the SOA, ϕ is the effective quantum yield, defined here as the number of carbons lost per photon absorbed and assumed to be independent of wavelength, I is the spectral actinic flux (photons cm^{-2} s^{-1} nm^{-1}), and λ is the wavelength (nanometers). The c_{pM} and C_{frag} terms set J to the loss rate of carbon, as opposed to the loss rate of molecules (the more standard formulation of J, typically used to describe the photolysis of gas-phase molecules).

Determination of f_R and τ from the fit to the time-dependent loss of particulate carbon (eq 1) allows the number of chromophores per molecule (c_{pM}) and the effective quantum yield (ϕ) to be determined from eqs 2 and 3, assuming the other parameters [C_{frag}, C_{tot}, $\sigma(\lambda)$, and $I(\lambda)$]. Here, the absorption cross section for α-pinene SOA from Wong et al.[7] and the photon flux from the UVA lamps in the chamber were used (Figure S5) for $\sigma(\lambda)$ and $I(\lambda)$, respectively. Previous studies provide some initial constraints on the other parameters. The range of carbon numbers measured in α-pinene SOA is ∼8−19, with the most abundant product observed, pinic acid, a C9 compound;[26] we thus set C_{tot} to be

DOI: 10.1021/acs.jpclett.9b01417
J. Phys. Chem. Lett. 2019, 10, 4003−4009

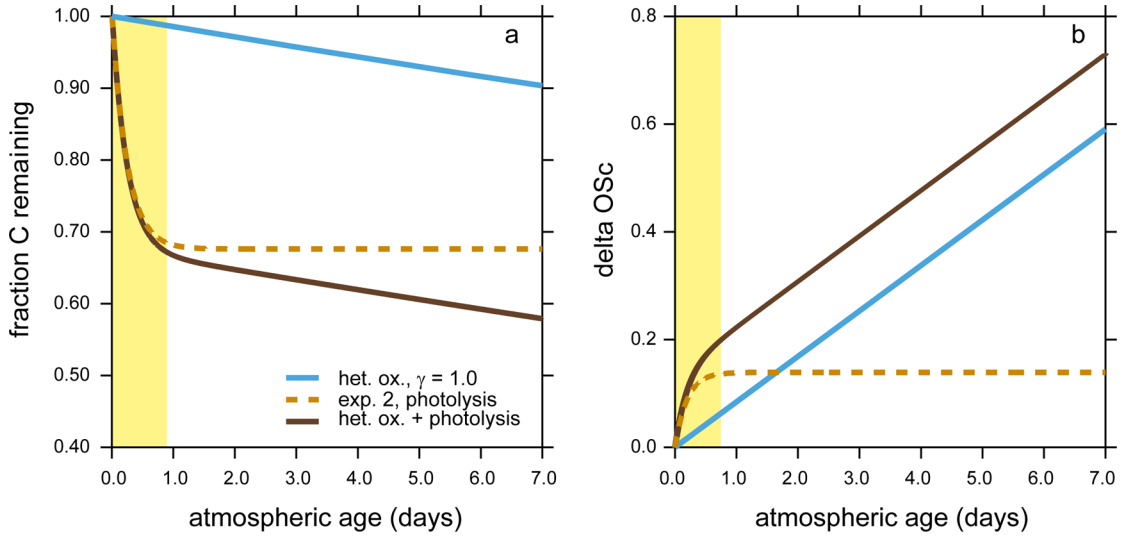

Figure 4. Predicted changes to atmosperhic OA with aging using experiment 1. (a) Fraction of carbon remaining and (b) net change in carbon oxidation state as a function of particle age for photolysis (light brown dashed line) and heterogeneous oxidation (blue solid line).[3] The net change (photolysis and heterogeneous oxidation) is shown by the dark brown solid line. The shaded region shows the initial time period where photolysis is dominant; thereafter, other atmospheric aging mechanisms will drive changes in f_C and $\overline{OS}_C$. Experiments 2 and 3 show similar trends with small differences in the total extent of change due to photolysis (Figure S6).

9 carbon atoms. Volatile fragments observed from SOA photolysis range from 1 to 3 carbon atoms,[9] so a value of 2.2 carbon atoms is assumed for C_{frag}. Using these values, we determine c_{pM} values of 0.7−1 chromophore per SOA molecule, with an effective quantum yield of 1.5−3 (Table 1). If the average molecular size (C_{tot}) is larger than our assumed value, then the derived values for both ϕ and c_{pM} are higher than those listed in Table 1 (Figure S4). When the units for the quantum yield are converted to the number of molecules per photon, the quantum yields estimated from the first two experiments (~1.0) are similar to the quantum yield estimated by Wong et al. of 1.2 ± 0.2, despite being calculated using different approaches.[7]

The fitted parameters (Table 1) suggest that the molecules formed at higher loadings of SOA (experiments 1 and 2) have more chromophores than those in lower loadings of SOA (experiment 3). For lower OA loading (experiment 3), a larger fraction of molecules with either one or no chromophores is present. These differences may be driven by volatility differences, or they may be due to chemical differences in the type and amount of oligomers formed. These simulations provide initial constraints on variables that can be used to predict SOA photolytic mass loss rates and extents in the atmosphere when a fraction of the SOA mass is photo-recalcitrant.

By extrapolating changes in f_C and $\Delta\overline{OS}_C$ to atmospheric lifetimes, we can evaluate and compare the long time scale impact of photolysis on SOA to the effects of other atmospheric aging processes. Figure 4 shows these trends combined with predicted changes as a result of heterogeneous oxidation via OH radicals.[3] Here, the same scaling factor for atmospheric UV exposure used in Figure 2 has been applied. Both photolysis and heterogeneous oxidation can have substantial impacts on the chemical properties of α-pinene SOA, but they occur on very different time scales. Photolysis drives an initial, rapid decrease in the carbon fraction and an increase in the oxidation state over the first day. After this, its impact decreases considerably and heterogeneous oxidation (and possibly other aging mechanisms, as well) becomes dominant.

Overall, this work demonstrates that treatments of photolytic SOA mass loss should account for a substantial photo-recalcitrant mass fraction. A detailed understanding of the photolytic fate of SOA will require additional experimental studies, spanning a range of chemical systems and reaction conditions. Most importantly, this work should be extended to cover different types of SOA, generated and photolytically aged under a variety of ambient conditions (temperature, RH, OA loading, with and without oxidants or radical species, etc.). These data can be supplemented with more detailed chemical measurements, providing information about the identity and number of chromophores in SOA as well as the identity of the volatile products. In addition, the effects of photolysis on the chemical and physical properties of the particles should be probed. Photolysis rates have been shown to depend on viscosity,[27,28] likely in part due to a slowing or quenching of the excited state in the particle phase.[5] Here, we show that the photolysis-driven mass loss rate and recalcitrant fraction of SOA can be predicted with values for the average number of chromophores, the size of the fragments, the size of the parent molecule, and the quantum yield. In addition, experiments that access higher photon exposures (via longer time scale experiments and/or higher photon fluxes) will enable analysis of the photolytic fate of SOA beyond the ~1−2 days of photolysis accessed in our study.

In the atmosphere, photolysis changes the SOA mass and composition over the first day, after which the SOA is effectively photobleached and other aging/loss processes will dominate. This simple framework assumes an initial chromophore population. However, heterogeneous oxidation (and possibly other oxidative processes, such as aqueous-phase oxidation) can lead to functionalization of particulate organic carbon, which may include production of new chromophores.[38] Thus, in the atmosphere, the significantly slower photolysis mass loss rate observed here at longer times may be balanced by the new chromophores formed via these oxidation

DOI: 10.1021/acs.jpclett.9b01417
J. Phys. Chem. Lett. 2019, 10, 4003−4009

processes. On the other hand, these oxidative processes can also degrade or remove chromophores from the particulate mass, potentially increasing the mass fraction of SOA that is photo-recalcitrant.[36,39,40] The effects of all of these aging processes are likely to vary with the chemical composition as well as ambient conditions such as RH and temperature.[7,27,28,41] Future studies that probe the interactions and feedbacks between all chemical aging/loss processes, under different ambient conditions and for different SOA precursors, are needed to improve our understanding of the life cycle of atmospheric organic aerosol.

■ ASSOCIATED CONTENT

Supporting Information

The Supporting Information is available free of charge on the ACS Publications website at DOI: 10.1021/acs.jpclett.9b01417.

Expanded methods and data sets for chamber experiments, model calculations, and light fluxes (PDF)

■ AUTHOR INFORMATION

Corresponding Author

*E-mail: reobrien@wm.edu.

ORCID

Rachel E. O'Brien: 0000-0001-8829-5517

Author Contributions

R.E.O. and J.H.K. designed the experiments, and R.E.O. carried out the experiments. The manuscript was written by R.E.O. with extensive input from J.H.K. Both authors have given approval to the final version of the manuscript.

Notes

The authors declare no competing financial interest.

■ ACKNOWLEDGMENTS

This work was supported by National Science Foundation Grant AGS-1638672 and National Oceanic and Atmospheric Administration Grants NA13OAR4310072 and NA140AR4310132.

■ REFERENCES

(1) Heald, C. L.; Coe, H.; Jimenez, J. L.; Weber, R. J.; Bahreini, R.; Middlebrook, A. M.; Russell, L. M.; Jolleys, M.; Fu, T.-M.; Allan, J. D.; et al. Exploring the Vertical Profile of Atmospheric Organic Aerosol: Comparing 17 Aircraft Field Campaigns with a Global Model. *Atmos. Chem. Phys.* **2011**, *11*, 12673−12696.

(2) Hodzic, A.; Kasibhatla, P. S.; Jo, D. S.; Cappa, C. D.; Jimenez, J. L.; Madronich, S.; Park, R. J. Rethinking the Global Secondary Organic Aerosol (SOA) Budget: Stronger Production, Faster Removal, Shorter Lifetime. *Atmos. Chem. Phys.* **2016**, *16*, 7917−7941.

(3) Kroll, J. H.; Lim, C. Y.; Kessler, S. H.; Wilson, K. R. Heterogeneous Oxidation of Atmospheric Organic Aerosol: Kinetics of Changes to the Amount and Oxidation State of Particle-Phase Organic Carbon. *J. Phys. Chem. A* **2015**, *119*, 10767−10783.

(4) Daumit, K. E.; Carrasquillo, A. J.; Sugrue, R. A.; Kroll, J. H. Effects of Condensed-Phase Oxidants on Secondary Organic Aerosol Formation. *J. Phys. Chem. A* **2016**, *120*, 1386−1394.

(5) Henry, K. M.; Donahue, N. M. Photochemical Aging of α-Pinene Secondary Organic Aerosol: Effects of OH Radical Sources and Photolysis. *J. Phys. Chem. A* **2012**, *116*, 5932−5940.

(6) Malecha, K. T.; Cai, Z.; Nizkorodov, S. A. Photodegradation of Secondary Organic Aerosol Material Quantified with a Quartz Crystal Microbalance. *Environ. Sci. Technol. Lett.* **2018**, *5*, 366−371.

(7) Wong, J. P. S.; Zhou, S.; Abbatt, J. P. D. Changes in Secondary Organic Aerosol Composition and Mass Due to Photolysis: Relative Humidity Dependence. *J. Phys. Chem. A* **2015**, *119*, 4309−4316.

(8) Epstein, S. A.; Blair, S. L.; Nizkorodov, S. A. Direct Photolysis of A-pinene Ozonolysis Secondary Organic Aerosol: Effect on Particle Mass and Peroxide Content. *Environ. Sci. Technol.* **2014**, *48*, 11251−11258.

(9) Malecha, K. T.; Nizkorodov, S. A. Photodegradation of Secondary Organic Aerosol Particles as a Source of Small, Oxygenated Volatile Organic Compounds. *Environ. Sci. Technol.* **2016**, *50*, 9990−9997.

(10) Kroll, J. H.; Ng, N. L.; Murphy, S. M.; Flagan, R. C.; Seinfeld, J. H. Secondary Organic Aerosol Formation from Isoprene Photooxidation. *Environ. Sci. Technol.* **2006**, *40*, 1869−1877.

(11) Presto, A. A.; Huff Hartz, K. E.; Donahue, N. M. Secondary Organic Aerosol Production from Terpene Ozonolysis. 1. Effect of UV Radiation. *Environ. Sci. Technol.* **2005**, *39*, 7036−7045.

(12) Hodzic, A.; Madronich, S.; Kasibhatla, P. S.; Tyndall, G.; Aumont, B.; Jimenez, J. L.; Lee-Taylor, J.; Orlando, J. Organic Photolysis Reactions in Tropospheric Aerosols: Effect on Secondary Organic Aerosol Formation and Lifetime. *Atmos. Chem. Phys.* **2015**, *15*, 9253−9269.

(13) Aiona, P. K.; Luek, J. L.; Timko, S. A.; Powers, L. C.; Gonsior, M.; Nizkorodov, S. A. Effect of Photolysis on Absorption and Fluorescence Spectra of Light-Absorbing Secondary Organic Aerosols. *ACS Earth Sp. Chem.* **2018**, *2*, 235−245.

(14) Wang, X.; Heald, C. L.; Sedlacek, A. J.; De Sá, S. S.; Martin, S. T.; Alexander, M. L.; Watson, T. B.; Aiken, A. C.; Springston, S. R.; Artaxo, P. Deriving Brown Carbon from Multiwavelength Absorption Measurements: Method and Application to AERONET and Aethalometer Observations. *Atmos. Chem. Phys.* **2016**, *16*, 12733−12752.

(15) Forrister, H.; Liu, J.; Scheuer, E.; Dibb, J.; Ziemba, L.; Thornhill, K. L.; Anderson, B.; Diskin, G.; Perring, A. E.; Schwarz, J. P.; et al. Evolution of Brown Carbon in Wildfire Plumes. *Geophys. Res. Lett.* **2015**, *42*, 4623−4630.

(16) Zhao, R.; Lee, A. K. Y.; Huang, L.; Li, X.; Yang, F.; Abbatt, J. P. D. Photochemical Processing of Aqueous Atmospheric Brown Carbon. *Atmos. Chem. Phys.* **2015**, *15*, 6087−6100.

(17) Hunter, J. F.; Carrasquillo, A. J.; Daumit, K. E.; Kroll, J. H. Secondary Organic Aerosol Formation from Acyclic, Monocyclic, and Polycyclic Alkanes. *Environ. Sci. Technol.* **2014**, *48*, 10227−10234.

(18) Decarlo, P. F.; Kimmel, J. R.; Trimborn, A.; Northway, M. J.; Jayne, J. T.; Aiken, A. C.; Gonin, M.; Fuhrer, K.; Horvath, T.; Docherty, K. S.; et al. Field-Depolyable, High-Resolution, Time-of-Flight Aerosol Mass Spectrometer. *Anal. Chem.* **2006**, *78* (24), 8281−8289.

(19) Mang, S. A.; Henricksen, D. K.; Bateman, A. P.; Sulbaek Andersen, M. P.; Blake, D. R.; Nizkorodov, S. A. Contribution of Carbonyl Photochemistry to Aging of Atmospheric Secondary Organic Aerosol. *J. Phys. Chem. A* **2008**, *112* (36), 8337−8344.

(20) Bateman, A. P.; Nizkorodov, S. a.; Laskin, J.; Laskin, A. Photolytic Processing of Secondary Organic Aerosols Dissolved in Cloud Droplets. *Phys. Chem. Chem. Phys.* **2011**, *13* (26), 12199−12212.

(21) Ehn, M.; Thornton, J. A.; Kleist, E.; Sipilä, M.; Junninen, H.; Pullinen, I.; Springer, M.; Rubach, F.; Tillmann, R.; Lee, B.; et al. A Large Source of Low-Volatility Secondary Organic Aerosol. *Nature* **2014**, *506*, 476−479.

(22) Zhang, X.; Lambe, A. T.; Upshur, M. A.; Brooks, W. A.; Gray Bé, A.; Thomson, R. J.; Geiger, F. M.; Surratt, J. D.; Zhang, Z.; et al. Highly Oxygenated Multifunctional Compounds in α-Pinene Secondary Organic Aerosol. *Environ. Sci. Technol.* **2017**, *51*, 5932−5940.

(23) Krapf, M.; El Haddad, I.; Bruns, E. A.; Molteni, U.; Daellenbach, K. R.; Prévôt, A. S. H.; Baltensperger, U.; Dommen, J. Labile Peroxides in Secondary Organic Aerosol. *Chem.* **2016**, *1* (4), 603−616.

DOI: 10.1021/acs.jpclett.9b01417
J. Phys. Chem. Lett. 2019, 10, 4003−4009

(24) Lee, H. J.; Aiona, P. K.; Laskin, A.; Laskin, J.; Nizkorodov, S. A. Effect of Solar Radiation on the Optical Properties and Molecular Composition of Laboratory Proxies of Atmospheric Brown Carbon. *Environ. Sci. Technol.* **2014**, *48*, 10217−10226.
(25) Zhong, M.; Jang, M. Dynamic Light Absorption of Biomass-Burning Organic Carbon Photochemically Aged under Natural Sunlight. *Atmos. Chem. Phys.* **2014**, *14*, 1517−1525.
(26) Zhang, X.; Mcvay, R. C.; Huang, D. D.; Dalleska, N. F.; Aumont, B.; Flagan, R. C.; Seinfeld, J. H. Formation and Evolution of Molecular Products in α-Pinene Secondary Organic Aerosol. *Proc. Natl. Acad. Sci. U. S. A.* **2015**, *112*, 14168−14173.
(27) Lignell, H.; Hinks, M. L.; Nizkorodov, S. A. Exploring Matrix Effects on Photochemistry of Organic Aerosols. *Proc. Natl. Acad. Sci. U. S. A.* **2014**, *111*, 13780−13785.
(28) Hinks, M. L.; Brady, M. V.; Lignell, H.; Song, M.; Grayson, J. W.; Bertram, A. K.; Lin, P.; Laskin, A.; Laskin, J.; Nizkorodov, S. A. Effect of Viscosity on Photodegradation Rates in Complex Secondary Organic Aerosol Materials. *Phys. Chem. Chem. Phys.* **2016**, *18*, 8785−8793.
(29) Donahue, N. M.; Robinson, A. L.; Trump, E. R.; Riipinen, I.; Kroll, J. H. Volatility and Aging of Atmospheric Organic Aerosol. *Top. Curr. Chem.* **2012**, *339*, 97−143.
(30) Chan, M. N.; Chan, A. W. H.; Chhabra, P. S.; Surratt, J. D.; Seinfeld, J. H. Modeling of Secondary Organic Aerosol Yields from Laboratory Chamber Data. *Atmos. Chem. Phys.* **2009**, *9*, 5669−5680.
(31) Kroll, J. H.; Seinfeld, J. H. Chemistry of Secondary Organic Aerosol: Formation and Evolution of Low-Volatility Organics in the Atmosphere. *Atmos. Environ.* **2008**, *42*, 3593−3624.
(32) Shilling, J. E.; Chen, Q.; King, S. M.; Rosenoern, T.; Kroll, J. H.; Worsnop, D. R.; Decarlo, P. F.; Aiken, A. C.; Sueper, D.; Jimenez, J. L.; et al. Loading-Dependent Elemental Composition of α-Pinene SOA Particles. *Atmos. Chem. Phys.* **2009**, *9*, 771−782.
(33) Day, D. A.; Liu, S.; Russell, L. M.; Ziemann, P. J. Organonitrate Group Concentrations in Submicron Particles with High Nitrate and Organic Fractions in Coastal Southern California. *Atmos. Environ.* **2010**, *44*, 1970−1979.
(34) Coury, C.; Dillner, A. M. ATR-FTIR Characterization of Organic Functional Groups and Inorganic Ions in Ambient Aerosols at a Rural Site. *Atmos. Environ.* **2009**, *43*, 940−948.
(35) Kroll, J. H.; Donahue, N. M.; Jimenez, J. L.; Kessler, S. H.; Canagaratna, M. R.; Wilson, K. R.; Altieri, K. E.; Mazzoleni, L. R.; Wozniak, A. S.; Bluhm, H.; et al. Carbon Oxidation State as a Metric for Describing the Chemistry of Atmospheric Organic Aerosol. *Nat. Chem.* **2011**, *3*, 133−139.
(36) Daumit, K. E.; Carrasquillo, A. J.; Hunter, J. F.; Kroll, J. H. Laboratory Studies of the Aqueous-Phase Oxidation of Polyols: Submicron Particles vs. Bulk Aqueous Solution. *Atmos. Chem. Phys.* **2014**, *14*, 10773−10784.
(37) Donahue, N. M.; Henry, K. M.; Mentel, T. F.; Kiendler-Scharr, A.; Spindler, C.; Bohn, B.; Brauers, T.; Dorn, H. P.; Fuchs, H.; Tillmann, R.; et al. Aging of Biogenic Secondary Organic Aerosol via Gas-Phase OH Radical Reactions. *Proc. Natl. Acad. Sci. U. S. A.* **2012**, *109*, 13503−13508.
(38) Kroll, J. H.; Smith, J. D.; Che, D. L.; Kessler, S. H.; Worsnop, D. R.; Wilson, K. R. Measurement of Fragmentation and Functionalization Pathways in the Heterogeneous Oxidation of Oxidzed Organic Aerosol. *Phys. Chem. Chem. Phys.* **2009**, *11*, 8005−8014.
(39) Hems, R. F.; Abbatt, J. P. D. Aqueous Phase Photo-Oxidation of Brown Carbon Nitrophenols: Reaction Kinetics, Mechanism, and Evolution of Light Absorption. *ACS Earth Sp. Chem.* **2018**, *2*, 225−234.
(40) Mysak, E. R.; Smith, J. D.; Ashby, P. D.; Newberg, J. T.; Wilson, K. R.; Bluhm, H. Competitive Reaction Pathways for Functionalization and Volatilization in the Heterogeneous Oxidation of Coronene Thin Films by Hydroxyl Radicals and Ozone. *Phys. Chem. Chem. Phys.* **2011**, *13*, 7554−7564.
(41) Li, Z.; Smith, K. A.; Cappa, C. D. Influence of Relative Humidity on the Heterogeneous Oxidation of Secondary Organic Aerosol. *Atmos. Chem. Phys.* **2018**, *18*, 14585−14608.

NOTE ADDED AFTER ASAP PUBLICATION

Due to production error, Table 1 footnote was omitted in the version published on July 5, 2019. It was correctly restored on July 10, 2019.

DOI: 10.1021/acs.jpclett.9b01417
J. Phys. Chem. Lett. 2019, 10, 4003−4009